

# Journal of Materials Chemistry B

Accepted Manuscript



This is an *Accepted Manuscript*, which has been through the Royal Society of Chemistry peer review process and has been accepted for publication.

*Accepted Manuscripts* are published online shortly after acceptance, before technical editing, formatting and proof reading. Using this free service, authors can make their results available to the community, in citable form, before we publish the edited article. We will replace this *Accepted Manuscript* with the edited and formatted *Advance Article* as soon as it is available.

You can find more information about *Accepted Manuscripts* in the [Information for Authors](#).

Please note that technical editing may introduce minor changes to the text and/or graphics, which may alter content. The journal's standard [Terms & Conditions](#) and the [Ethical guidelines](#) still apply. In no event shall the Royal Society of Chemistry be held responsible for any errors or omissions in this *Accepted Manuscript* or any consequences arising from the use of any information it contains.

## ARTICLE

## Localized drug delivery of selenium (Se) using nanoporous anodic aluminium oxide for bone implants

Full Cite this: DOI: 10.1039/x0xx00000x

Received 00th January 2012,  
Accepted 00th January 2012

DOI: 10.1039/x0xx00000x

www.rsc.org/

Viswanathan S. Saji,<sup>a</sup> Tushar Kumeria,<sup>a</sup> Karan Gulati,<sup>a</sup> Matthew Prideaux,<sup>b</sup> Shafiur Rahman,<sup>a</sup> Mohammed Alsawat,<sup>a</sup> Abel Santos,<sup>a</sup> Gerald J. Atkins,<sup>b</sup> and Dusan Losic<sup>\*a</sup>

Electrochemically engineered nanoporous anodized aluminium oxide (AAO) prepared on aluminium (Al) foil by anodization process was employed as a platform for different forms of selenium (Se) in order to investigate their release behaviour and potential application for localized drug delivery targeting bone cancer. Several forms of Se including inorganic Se ( $\text{H}_2\text{SeO}_3$ ), organic Se ( $(\text{C}_6\text{H}_5)_2\text{Se}$ ), metallic Se, their chitosan composites, electrodeposited (ED) and chemical vapour deposited (CVD) Se were explored and combined with another model drug (indomethacin). Structural, drug-loading and in-vitro drug-releasing characteristics of prepared Se-based drug delivery carriers were characterized by Scanning Electron Microscopy (SEM), Thermogravimetric Analysis (TGA) and UV-Visible Spectroscopy (UV-Vis), respectively. Sustained and controlled release of Se was demonstrated through chitosan-composites of inorganic, organic or metallic forms of Se loaded into nanoporous AAO carriers. Cell viability studies showed decreasing toxicity to cancer cells in the order: inorganic Se > ED Se > CVD Se > metallic Se > organic Se. The study suggests new alternatives for localized drug treatment based on low-cost nano-engineered carriers loaded with Se having anti-cancer properties.

### Introduction

Osteosarcoma is the most prevalent type of malignant bone cancer (sixth most frequently occurring cancer in children and young adults). The overall survival rate of patients suffering from osteosarcoma is approximately 60-70 % if subjected to multi-agent chemotherapy followed by surgery.<sup>1-2</sup> Despite remarkable research in this field, no major turnaround in treatment and outcome has been achieved.

A major concern in therapies associated with bone cancer is an increased risk of cancer recurrence.<sup>3</sup> Selenium (Se) therapy is important in this regard and can help in post-surgery cancer treatment by reducing the likelihood of cancer recurrence. Se is known to function as an anti-oxidant and is relevant for a number of chronic diseases linked to oxidative stress.<sup>4-6</sup> Twenty five selenoproteins have been identified in the human proteome that exhibit anti-oxidant activities. Demographic data have indicated a decreased cancer risk in regions with elevated soil levels of Se.<sup>4</sup> Supra-nutritional supplements of 200-400 mg of Se per day have been shown to provide chemo-preventative benefits against several forms of cancer.<sup>7,8</sup> A number of novel Se compounds have been reported as key components of anti-cancer drugs.<sup>9,10</sup> Several recent studies focussed on nanoscale

Se for cancer chemoprevention were reported.<sup>11-16</sup> Yang et al. showed that surface functionalization of Se nanoparticles with Spirulina-polysaccharides significantly enhanced its cellular uptake and cytotoxicity toward several human cancer cell lines.<sup>12</sup> Medical benefits and potential advantages of Se for biomedical applications are summarized in **Figure S1 (Supplementary information)**.

Se can exist in variety of allotropic forms such as metallic hexagonal gray, deep red monoclinic, red, black or brown amorphous forms or vitreous forms. The principal oxidation states of Se are +VI (selenate) +IV (selenite), 0 (elemental Se) and -II (selenide).<sup>17</sup> The inorganic forms of Se with oxidation state of +VI and +IV have been shown to have cytotoxic effects on several human cancer cell lines, whereas elemental Se is generally considered nontoxic due to its insolubility.<sup>18</sup> Organic forms of Se have also been studied for their biological effects.<sup>7</sup>

Most of the previous pharmaceutical studies were based on systemic drug delivery of Se, which has limitations due to side effects and potential toxicity of Se at higher dosages. Surprisingly, only one study considered the use of localized drug delivery, where the authors employed electrodeposited Se in anodized titanium nanotubes (TNTs).<sup>19</sup> However, the disadvantage of this concept is the loading of Se into TNTs implant by the electrodeposition process, which is complicated

and requires an additional metal coating compared to conventional drug-loading using simple solutions of Se salts or organic Se compounds. Therefore exploring different forms of Se with controllable drug-release for localized drug delivery is an important potential approach for cancer therapy.

Local drug delivery using nanoporous implants is an attractive option to overcome the limitations of conventional drug delivery such as poor bioavailability, lack of selectivity, limited drug solubility, low drug effectiveness and inappropriate pharmacokinetics.<sup>20-24</sup> Among the different nanoporous substrates investigated for localized drug delivery, anodized porous oxides of titanium (Ti) and aluminium (Al) has attracted a great deal of recent research interest because of low cost of fabrication, controllable pore structure, tailored surface chemistry, high surface area, high loading capability, chemical resistivity, mechanical rigidity and excellent biocompatibility.<sup>21-24</sup>

In this study we employed electrochemically engineered anodized aluminium oxide (AAO) as a model nanoporous drug delivery carrier and investigated the release behaviour of various forms of Se and their toxicity for cancer cells. Several recent studies investigated nanoporous AAO for various biomedical applications.<sup>25-28</sup> Five different forms of loaded Se (with or without chitosan) into AAO implants, including inorganic Se ( $\text{H}_2\text{SeO}_3$ ), organic Se ( $(\text{C}_6\text{H}_5)_2\text{Se}$ ), metallic Se (Se), electrodeposited (ED) Se and chemical vapour deposited (CVD) Se (**Figure 1**) were explored and compared for their drug-release performance and cancer cell toxicity. The objective was to explore drug-releasing behaviour of Se from nanoporous drug delivery system using different sources of Se (inorganic selenite salt, organic diselenide compound, metallic Se, ED amorphous Se and CVD crystalline Se). More specifically, we focused on developing an optimised drug delivery system with sustained and controlled drug-release using single and multi-drug delivery system combined with chitosan (an established antibacterial agent and promoter of osseointegration) and indomethacin (model drug) loading. The significance of this work is to demonstrate new alternatives for cancer therapy based on localized drug delivery systems using simple nano-engineered carriers and low-cost therapeutics based on Se.

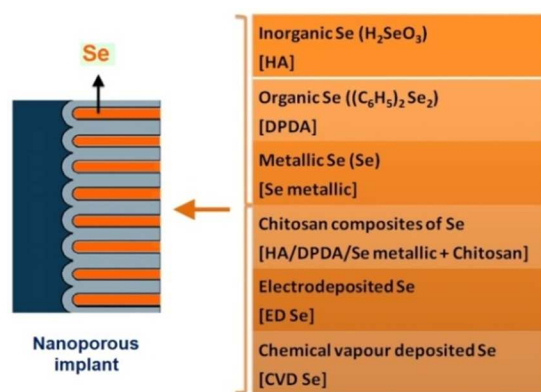


**Fig. 1** Summary of explored nanoporous drug delivery systems using different sources of Se.

## Experimental

High purity (99.7%) Al sheets (thickness 0.75 mm) supplied by Alfa Aesar (Ward Hill, MA) were used as the substrate

material. Selenous acid ( $\text{H}_2\text{SeO}_3$ , 98.0 %), diphenyl diselenide ( $(\text{C}_6\text{H}_5)_2\text{Se}$ , 98.0 %), Se pellet (~ 2mm, metal basis, 99.9 %), phosphate-buffered saline (PBS), chitosan, indomethacin, oxalic acid ( $\text{H}_2\text{C}_2\text{O}_4$ ), copper (II) chloride dihydrate ( $\text{CuCl}_2 \cdot 2\text{H}_2\text{O}$ ), chromium trioxide ( $\text{CrO}_3$ ), HCl and  $\text{H}_3\text{PO}_4$  were purchased from Sigma-Aldrich (Sydney). High purity Milli-Q water (18.2 M $\Omega$ ) sieved through a 0.22  $\mu\text{m}$  filter was used.

### Fabrication of nanoporous AAO as drug-releasing carrier

AAO samples were prepared by the well known two step anodization method,<sup>29</sup> using 0.3 M oxalic acid solution. The area exposed for anodization was 1  $\text{cm}^2$ . The Al sheet was cut into equal lengths of ~ 1.5  $\text{cm}^2$  each, mechanically polished and cleaned by sonication in acetone for 30 min prior to anodization. Anodization steps were performed using a specially designed electrochemical cell and computer-controlled power supply (Agilent, Santa Clara, CA). In the first anodization step, a constant voltage of 40 V was applied for 20 h at 6  $^\circ\text{C}$ . The obtained anodic AAO layer was removed by etching in  $\text{CrO}_3$ - $\text{H}_3\text{PO}_4$  solution, leaving the nano-textured Al surface. Second anodization was performed under the same voltage and temperature for 3 h and that was followed by a pore widening step in 5 %  $\text{H}_3\text{PO}_4$  for 15 min to yield AAO template with length of ~ 10  $\mu\text{m}$  and diameter of ~ 70 nm. Most of the experiments were conducted with AAO having Al base. A few experiments were also conducted after removing the Al base. A green solution of  $\text{CuCl}_2 \cdot 2\text{H}_2\text{O}$  (13.6 g) and HCl (100 mL) in 400 mL water was used for Al removal where a specially made cell set-up was used.

### Preparation of Se and their loading into nanoporous carrier

**Chitosan composites of HA and DPDA:** 0.01 M solutions of HA and DPDA were made in ethanol. 1 wt. % chitosan solution was made in 0.8 vol. % of acetic acid solution. Equal volumes of 0.01 M HA (or DPDA) and chitosan-acetic acid solutions were mixed and sonicated.

**Se metal-Chitosan solution:** A few Se gray pellets were crushed and a small portion sonicated with ethylenediamine solution. A selected volume of the dissolved Se was diluted with equal volume of ethanol to obtain a desired concentration of Se. A fixed volume of the above solution was poured into an equal volume of chitosan-acetic acid solution, resulting in a red coloured solution.

**Electrodeposition of Se:** A conventional two electrode set-up was used for electrochemical deposition. AAO was placed inside a specially fabricated cell with its surface exposed to electrolyte. An Al foil connected with Al base of AAO was connected to the negative terminal of a power supply. A Ti sheet was used as the counter electrode. The electrolyte was aqueous solution of 0.01 M  $\text{H}_2\text{SeO}_3$  + 0.5 M  $\text{Na}_2\text{SO}_4$ . Electrodeposition was performed at a selected voltage (4-8 V) for a selected duration (1-6 min) in order to achieve a desired Se deposition. Before deposition, a thin layer of gold (Au) was sputtered on AAO in order to make the surface conductive. A typical digital photograph of AAO after electrodeposition is provided in **Figure S<sub>2</sub>** (**Supplementary information**).

**Vapour deposition of Se:** A silica crucible containing crushed Se pellets (0.5-1 g) was used as the holder. AAO kept upside down inside the crucible in such a way that the circumference of AAO fits well with the periphery of crucible walls. The

crucible subsequently covered completely with Al foil and heated at 350 °C for 5-10 min in a tubular furnace under an Ar atmosphere and then cooled to room temperature. Care was taken that the Se vapour deposited evenly on the AAO. A typical Se-deposited AAO showed red colour formation (Figure S<sub>2</sub>, Supplementary information).

**Loading and release studies:** The release behaviour and cell toxicity of inorganic, organic and metallic forms of Se were investigated with and without chitosan composition and compared with that of ED and CVD Se. 1 wt. % of indomethacin in ethanol was used as model drug. Before loading, AAO was sonicated in ethanol and vacuum dried. The loading solution that included drug (i.e. indomethacin) was prepared by mixing the aforementioned solutions of chitosan, drug, and particular species of Se (i.e. HA, DPDA, or metallic Se) in 1:1:1 volumetric ratio. In a typical loading method, a few drops (approximately 10 μL) of loading solution were poured on AAO and kept in air for drying and the process repeated 8 times. After each step, the surface of AAO dried in air and gently cleaned with lint-free soft tissue. Se-only, Se-chitosan or drug-only samples were loaded similarly. The drug/Se loading efficiency was calculated by normalizing the amount loaded with the total amount of drug/Se used for loading (for drug, it is 800 μg, calculated for 8 drops of 1 wt. % of 10 μL solution). In a few experiments, Se was loaded with spin coating (2000 rpm, 30 s, 5 times) where a layer of chitosan-Se was spin coated on AAO. In ED and CVD Se, the corresponding processes namely electrodeposition and vapour deposition were employed for loading. The amount of loaded drug and Se in all samples was determined using Thermogravimetric Analysis (TGA, TA Instruments Q500). Additionally, BET analysis (Belsorp, Japan) of AAO before and after Se loading was carried out to study the surface area variation. Here, Al base of AAO was chemically removed and the remaining AAO layer was crushed into pieces to fit the glass tube for the measurement.

### Characterization

Structural characterization of prepared nanoporous AAO carriers before and after loading was performed using a field emission Scanning Electron Microscope (SEM, Philips XL 30) with thin film Energy Dispersive Spectroscopy (EDS) detector. The release characteristics were investigated using in-vitro studies in 20 mL 0.01 M PBS (pH 7.4) where the amount of released drug was measured using UV-Vis spectroscopy (Cary 60, Agilent). Measurements were taken at short intervals during first 8 h to monitor the initial burst release, followed by repeated measurements every 24 h to monitor the prolonged release into PBS. During each measurement, an aliquot of 3 mL was placed in a quartz cuvette and their absorbance measured to determine the released amount of drug or Se based on pre-constructed calibration curves. The cumulative mass release (via progressive addition of released amounts) were calculated and the % cumulative mass release [(cumulative mass release at a given time / total cumulative mass release) x 100] determined. Overall % mass release [(total cumulative mass release / total amount loaded) x 100] was used to determine the extent of drug release with respect to the amount loaded. Experiments were carried out in triplicate. The pH of solutions used for loading was adjusted to the range of 4-8 as AAO is structurally stable at the pH range of ~ 3-9. In certain experiments with CVD Se, variation of photoluminescence of AAO was studied as a function of time. Comparison of the

photoluminescence maximum before and after immersion of CVD Se deposited AAO in PBS provided a measure of Se release.

### Cell culture studies

Human primary osteoblast cells (NHBC) isolated as previously described,<sup>30</sup> and the human osteosarcoma cell line HOS (American Type Culture Collection, Rockville, MD, USA) were used to investigate the biocompatibility and cytotoxicity of Se containing AAO samples. Briefly, the cells were cultured in a modified minimal essential medium (Gibco) supplemented with ascorbate 2-phosphate (100 μM, Gibco), fetal calf serum (5 vol. %, Sigma) and penicillin (1 vol. %, Sigma) at 37 °C in 5 % CO<sub>2</sub>. AAO loaded with HA-chitosan, DPDA-chitosan, metallic Se-chitosan, ED Se and CVD Se were used as different test groups, including chitosan-loaded AAO, bare AAO and uncoated tissue culture plastic as controls. A typical Se/drug loaded AAO was cut into 4 equal sized pieces and one out of the four pieces was used in a group. All substrates were gas sterilized (ethylene oxide) and then placed in 48-well cell culture plates (Nunc). HOS and NHBC cells were removed from culture flasks using trypsin and combination of collagenase and dispase and resuspended at 1 × 10<sup>6</sup> cells/mL. An aliquot (50,000 cells) was added to each well containing test samples in separate plates and the plates were then incubated for 72 h at 37 °C. Cell growth was monitored and cell viability assessed using a crystal violet method.<sup>31</sup> For this, the medium was removed and the cells were gently rinsed twice with PBS. Attached cells were fixed with 200 μL of 10 % buffered formalin for 5-10 min, followed by washing twice with PBS. The samples were stained with 2-3 drops of 1 % (w/v) crystal violet solution for 20 min. After staining and incubation, the excess stain was removed by washing in water. After air-drying, the cell-associated stain was extracted with acetic acid (10 vol. %, 200 μL/well) for 20 min and the absorbance at 570 nm was measured by UV-Vis. We also measured the IC<sub>50</sub> value of the water soluble form of Se (i.e. HA) against HOS cells by incubating the HOS cells with different concentrations of HA (1 μM to 100 mM) and measuring the cell viability using bicinchoninic acid assay (Pierce<sup>TM</sup> BCA protein assay). A detailed protocol is provided in **Supplementary information**.

## Results and discussion

### Nanoporous AAO carrier and Se loading

A typical structure of prepared nanoporous AAO used as carriers for Se loading is presented in **Figure 2**. In this study, we prepared AAO with thickness of ~ 10 μm and diameter of ~ 70 nm, as confirmed by SEM characterization.

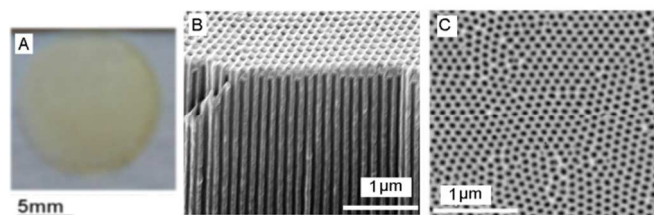


**Fig. 2** (A) Photograph of an entire AAO prepared on Al foil and (B & C) SEM images showing cross-section and top surface showing pore diameter.

It is worth noting that this is a scalable and low-cost fabrication process that can be applied to different forms of existing medical implants (needles, wires, plates) and used as drug releasing implants for localized drug delivery of therapeutics

Cross-sectional images of AAO loaded with different forms of Se and drug taken after loading are summarized in **Figure 3**. The images recorded for Se without chitosan mixing suggested that the re-crystallised Se particles attach to the pore walls of AAO (**Figures 3A & 3B**). The corresponding images after loading of Se-chitosan solutions of HA and DPDA (**Figures 3C & 3D**), however, showed a film-like formation inside the pore walls, suggesting that Se-chitosan solutions can more effectively infiltrate the porous framework. When Se-chitosan solution was spin coated, the film formation inside the pore walls was more evident (**Figure 3E**) with the formation of ~100 nm thick chitosan-Se film on the AAO surface (**Figure 3F**). **Figure 3G** shows a surface view image of ED Se. A typical view of CVD Se deposited AAO is shown in **Figure 3H**, where a few pores of AAO were found partially closed by the deposited Se. Both ED and CVD samples showed comparatively non-uniform distribution of deposited Se, whereas the chitosan composites of Se typically resulted in uniform loading within the porous network. The corresponding image of AAO after drug-loading is shown in **Figure 3I** where a thick deposit formation is evident throughout the porous network. Se loading is further confirmed by SEM-EDS (**Figure S3, Supplementary information**)

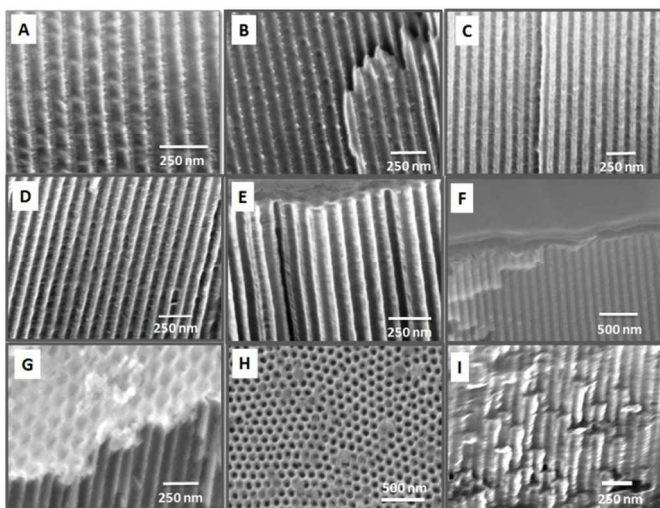


**Fig. 3** SEM images showing the nature of Se and drug-loading in AAO: (A) HA, (B) DPDA, (C) HA-chitosan, (D) DPDA-chitosan, (E, F) HA-chitosan (spin coated sample), (G) ED Se, (H) CVD Se and (I) drug (indomethacin) loaded sample. For (A)-(D) and (I), loading was performed after marginal bending.

Comparative TGA measurements were obtained and are presented in **Table 1** to show the relative amounts of the different types of Se and drug (indomethacin) loaded. The loading parameters of the different methods were adjusted with repeated experiments so that similar amounts of Se were loaded into the porous structure. A typical TGA plot showing the weight loss of Se loaded AAO is provided in **Figure S4 (Supplementary information)**. Note that the loading efficiency of drug (indomethacin) was calculated to be ~20% and we also calculated the loading ratio for different forms of

Se to drug as 2.12, 2.19, and 2.24 for HA : drug, DPDA : drug, and metallic Se : drug, respectively.

BET analysis of AAO before and after Se loading showed a significant reduction in surface area (i.e. bare AAO:  $1.402 \text{ m}^2\text{g}^{-1}$ , AAO + HA:  $0.119 \text{ m}^2\text{g}^{-1}$ , AAO + DPDA:  $0.035 \text{ m}^2\text{g}^{-1}$ ) (**Figure S5, Supplementary information**). The reduction in surface area and pore diameter is believed to be due to partial or complete blocking of AAO pores. The pore volume measured using BET was  $0.003527$ ,  $0.000594$ , and  $0.000523 \text{ cm}^3\text{g}^{-1}$  for bare AAO, AAO + HA, and AAO + DPDA, respectively. Similarly, the mean pore diameter was reduced from 69.58 nm for bare AAO to 40.74 and 38.48 nm for AAO + HA and AAO + DPDA, respectively.

### Drug-release studies from nanoporous AAO

In our initial experiments, we performed comprehensive UV-Vis spectroscopy study of different Se solutions in order to monitor their concentration and release from the AAO carrier (**Figure S6, Supplementary information**). As expected, different forms of Se solutions showed different wavelength range of absorption (see **Supplementary information**). Selection of a common wavelength for determination of released Se (from AAO) into PBS from different forms of loaded Se was therefore difficult. An earlier reported work used  $\lambda = 212 \text{ nm}$  (loading method was ED).<sup>19</sup> Hence, we compared the absorption of released Se into PBS at a number of selected wavelengths from  $\lambda = 200$  to 500 nm after different periods of release. A representative comparison of UV-Vis absorption is presented in **Figure 4**. It was interesting to see that irrespective of the disparity of loaded Se, the released Se showed a common absorption maximum at  $\lambda = 300 \text{ nm}$ . More information on spectral properties of Se,<sup>32,33</sup> and a concise literature analysis on UV-Vis absorption studies of Se,<sup>34-37</sup> are provided in **Supplementary information**.

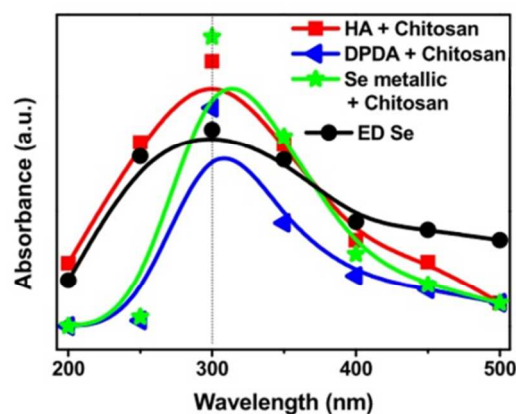


**Fig. 4** UV-Vis absorbance distribution of released Se into PBS. Absorbance values after 48 h of release from AAO were measured at selected wavelengths from 200 to 500 nm (connected by B-spline).

A similar wavelength of absorption maximum (**Figure 4**) suggested that the nature/size of released Se species (solvated Se species) into PBS can be the same irrespective of the dissimilarly loaded Se (see **Supplementary information**). Se has a lower solubility in PBS and hence its release can be mainly due to detachment from chitosan/AAO and that may be assisted by the biodegradability of chitosan. For HA, the released Se species will be solvated  $\text{SeO}_3^{2-}$  (HA is soluble in

PBS) where as for DPDA, the compound is expected to be released as such from biodegradable chitosan. Similarly, Se is expected to be released as such from metallic Se-chitosan, ED Se and CVD Se.

When HA or DPDA were loaded alone (without chitosan), the overall % mass release was only 10-15 % of the total amount loaded, and there was no appreciable release after 48 h (Table 1). Release from ED Se showed a similar trend to that of Se-chitosan solutions; however the cumulative mass release almost finished after 200 h (Figure 5). The extent of release from CVD Se was very low and that increased marginally with time (Table 1).

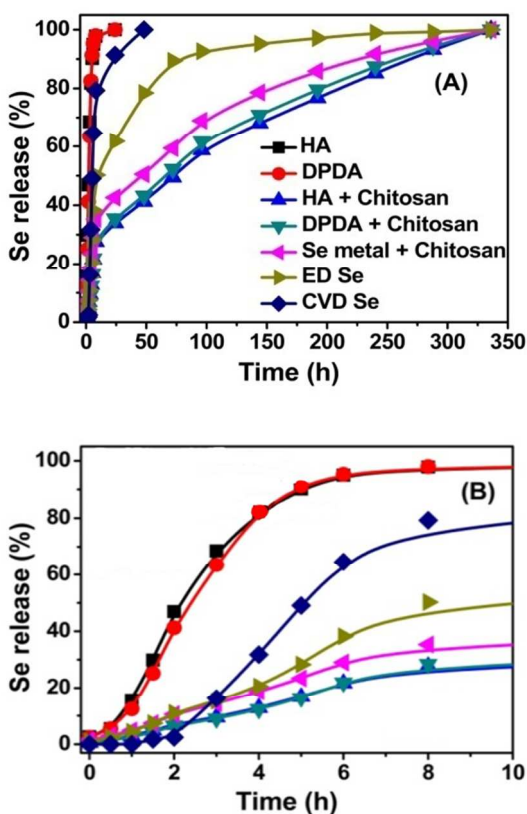


**Fig. 5** In-vitro Se release profiles of AAO loaded with different Se in PBS: (A) total cumulative; (B) burst cumulative and (C) cumulative mass release after 8, 100 and 300 h.  $\lambda_{\max}$  of Se at 300 nm was used. The values represent the means of at least three experiments.

ED causes deposition of amorphous Se(0) from Se(IV) electrolyte. When compared to Se-chitosan loadings, the overall % mass release for ED Se (~ 68 %) was less suggesting that a higher fraction of the loaded Se remained unreleased (Table 1), and that can be attributed to the strong adsorption of ED Se on AAO. However, during ED, loosely bound Se can form on AAO (as evident from SEM images) and this can be readily released. The amorphous nature of ED Se can also assist the release process. For CVD Se, red crystalline Se is formed on the surface and its release occurred at an extremely low rate (overall % mass release was ~ 1 % only) (Table 1). The crystalline red form of Se consists of mainly Se<sub>8</sub> ring molecules.<sup>38</sup> In general, at high temperatures; Se vapours consist of Se<sub>2</sub> molecules. As their temperature falls, they are polymerized into Se<sub>4</sub>, Se<sub>6</sub> and Se<sub>8</sub> molecules.<sup>38</sup> The lower overall % mass release of CVD Se (Table 1) can also be associated with the stronger adherence of the deposited Se owing to the high processing temperature. Alternatively, the chitosan-Se composites are expected to have the least adherence to AAO.

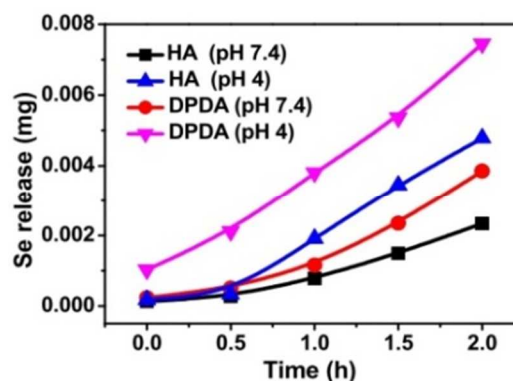


**Fig. 6** pH-dependent Se release from AAO

The influence of pH on release of selected Se loadings is presented in Figure 6. Even though Se release was very low (when loaded alone), it showed stimulated release at acidic pH levels. The release kinetics were high at pH 4 when compared to those at neutral pH, and this was true for all forms of Se used (with or without chitosan). A similar behaviour was observed when experiments were repeated at pH 4.5, 5 and 5.5 (not shown).

For CVD Se deposited AAO, the red colour of AAO marginally diminished after one week of immersion in acidic pH levels whereas the colour of sample immersed in neutral pH apparently remained unchanged. The photoluminescence variation of CVD Se deposited AAO as a function of pH level of PBS also provides an idea on the extent of Se release (Figures S7, Supplementary information).<sup>39</sup>

The following findings present the concept of multi-drug delivery by a combination of three therapeutic agents with different actions including indomethacin (antibiotic), Se (anti-cancer) and chitosan (anti-bacterial and osseointegration promoter). Figure 7 shows the release behaviour in this system with release graphs of the single drug (indomethacin) and in combination, when drug is loaded together with Se and chitosan. The % release of single drug (indomethacin) was significantly higher when compared to the corresponding Se-chitosan compositions and was proportional to the higher level of drug loaded (Table 1).

**Table 1** Amount loaded (by TGA) and cumulative mass release (by UV-Vis). The values represent the means of at least three experiments.

Type	Amount loaded (mg)	Cumulative mass release (mg) $\pm$ 0.003 (cumulative mass release in %)			Rate (mg/h) $\times 10^{-3}$		~ Overall % mass release
		8 h	48 h	100 h	Burst release	After 100 h	
HA - Chitosan	0.0632 $\pm$ 0.005	0.0162 (28 %)	0.0243 (41 %)	0.0348 (59 %)	2.0	0.35	92 %
DPDA - Chitosan	0.0624 $\pm$ 0.005	0.0144 (29 %)	0.0222 (43 %)	0.0315 (62 %)	1.8	0.32	84 %
Se metal - Chitosan	0.0648 $\pm$ 0.005	0.0210 (35 %)	0.0300 (50 %)	0.0408 (68 %)	2.6	0.41	90 %
ED Se	0.0521 $\pm$ 0.01	0.0141 (50 %)	0.0220 (76 %)	0.0279 (90 %)	1.8	0.28	68 %
CVD Se	0.0568 $\pm$ 0.01	0.0003 (79 %)	0.0008 (96 %)	0.0014 (99 %)	0.04	0.01	1 %
Drug (indomethacin)	0.1623 $\pm$ 0.02	0.0972 (64 %)	0.1140 (74 %)	0.1269 (80 %)	12.2	1.3	99 %
HA	0.0456 $\pm$ 0.005	0.0048 (97%)	0.0051 (99%)	-	0.6	-	13 %
DPDA	0.0486 $\pm$ 0.005	0.0090 (97%)	0.0094 (99%)	-	1.1	-	16 %

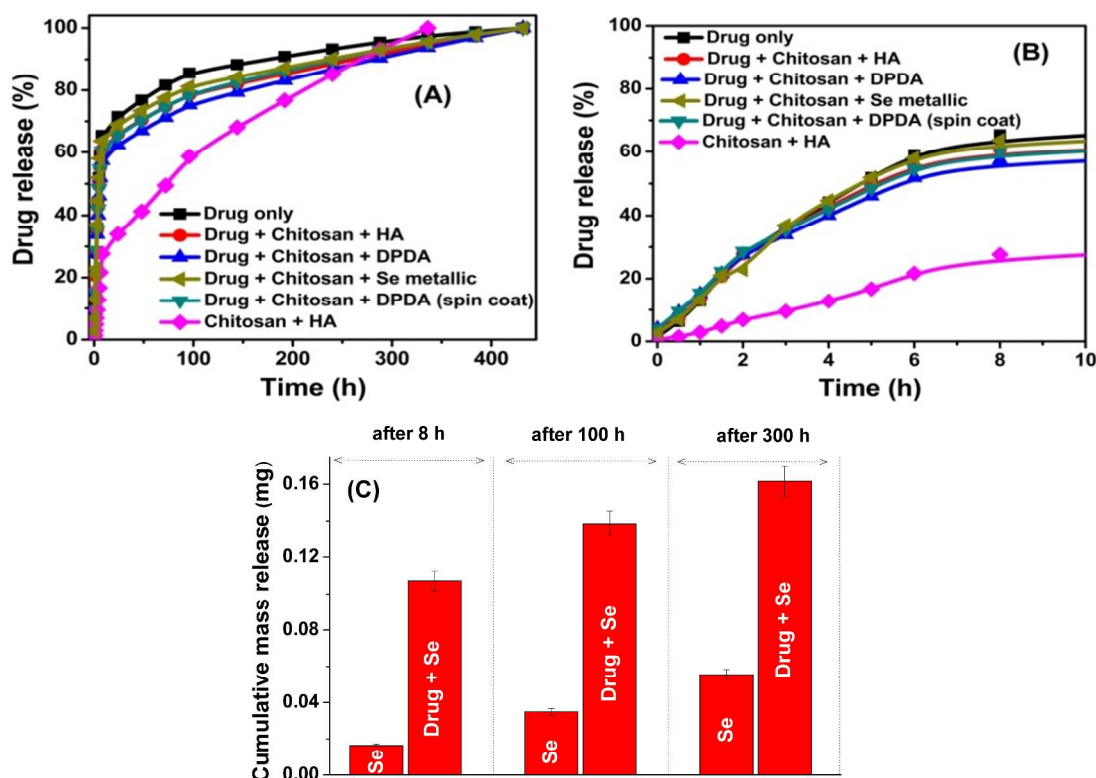


**Fig. 7** Multi drug (drug (indomethacin) + Se) release profiles: (A) total cumulative and (B) burst cumulative.  $\lambda_{\text{max}}$  of drug at 320 nm was used. Comparative variation of HA-chitosan is also provided. The values represent the means of at least three experiments. (C) Cumulative mass release of drug (from HA-chitosan-drug) and Se (from HA-chitosan) after 8, 100 and 300 h.

The difference in release of drug and Se-chitosan can be explained by differences in their solubility in buffer solution, which influences their diffusion rate into the bulk solution. The best-fitting model to the drug-release data was observed using Higuchi and zero-order release, which describes drug-release from an insoluble matrix.<sup>40</sup> The square root of a time-dependent process is based on the Fickian diffusion law, where the diffusion-controlled release rate of drug molecules decreases as a function of time due to a reduction in the concentration gradient.<sup>40</sup> The slow burst release of Se compared to indomethacin can be attributed to the strong adherence of Se to the pore walls and its low solubility. Se may also be adsorbed within the chitosan network.<sup>41</sup> Spin coating of Se-chitosan onto AAO in effect marginally reduced the extent of drug-release when compared to the corresponding solution-loaded sample (Figure 7). We have also compared drug-release from AAO after removing its Al base (Figure 8). As expected, on removing the Al base where the porous structure opened on both sides, the extent of burst release increased considerably.

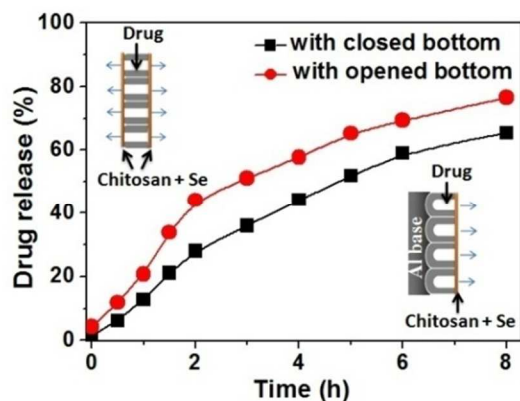


Fig. 8 Burst cumulative release of drug from AAO having closed bottom and opened bottom.

### Cell culture studies

Figure 9 depicts findings from cell culture studies using different Se loadings into the AAO carrier, where the % cell viability in osteosarcoma cells and primary osteoblastic cells are provided. Studies using HOS cells revealed an interesting comparison of the different forms of Se used, where the anti-cancer effect was found to be in the order: HA > ED Se > CVD Se > metallic Se > DPDA (Figure 9A).

Furthermore, we assessed the combination of HA with drug (indomethacin) for their ability to kill osteosarcoma cells. The results showed enhanced anticancer activity for AAO with co-loading of HA and drug in comparison to AAO loaded individually with HA or drug, thus, proving that this combination works in a synergistic manner. Interestingly, however, we noticed that HA loaded with chitosan performed best in comparison to all the other combinations, which could be due to the ability of chitosan to prevent the formation of an extracellular protein matrix layer.

Among the different mechanisms suggested for the anti-cancer effect of Se, such as reduction of oxidative stress,<sup>42</sup> promotion of apoptosis of cancer cells<sup>43</sup> and cancer cell DNA damage,<sup>44</sup> the effect based on its anti-oxidising ability and removal of reactive oxygen species (ROS) is the most accepted.<sup>42,45</sup> Se plays a key role in redox regulation as a modulator of ROS, such as superoxide, hydrogen peroxide and

hydroxyl radicals, which are constantly generated and eliminated in biological systems. Alternatively, Drake suggested that pro-oxidative rather than anti-oxidative properties of Se compounds best account for their anti-cancer effects.<sup>7</sup>

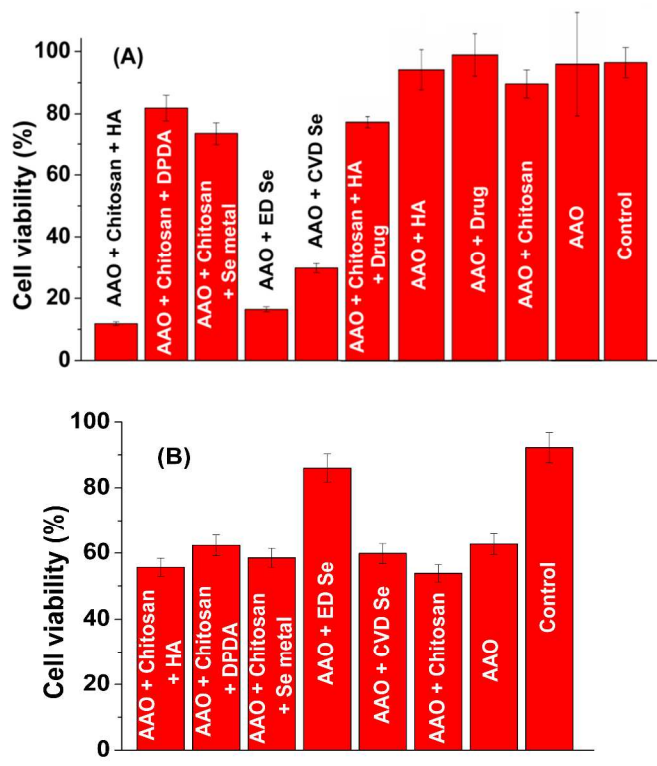


Fig. 9 Results of cell culture studies (% cell viability after 72 h of release) (A) HOS osteosarcoma cancer cells and (B) Primary osteoblast cells.

Generally, the inorganic form of Se with oxidation states of Se(IV) and Se(VI) are more toxic than organic Se that lack oxidation ability. Se(IV) is shown to be more toxic than Se(VI).<sup>7</sup> Se(IV) is expected to exert effects at low doses, directly oxidize critical cellular substrates, produce high steady-state levels of selenide anions and associated ROS and trigger apoptosis, and furthermore, are not removed from the metabolic Se pool by incorporation into proteins.<sup>7</sup> Comparison of the antitumor activity of a selenoamino acid (S-methylselenocysteine) with that of sodium selenite (Se(IV)) indicated that selenoaminoacids in concentration ranges of 50-200  $\mu\text{mol/L}$  are required to produce effects equivalent to those of selenite, which is active at much lower (1-10  $\mu\text{mol/L}$ ) concentrations.<sup>7</sup>

The properties of organic diselenides have received significant attention with the discovery that these compounds possess a mode of anti-oxidant action similar to that of glutathione peroxidase.<sup>46,47</sup> Other diselenides with anti-oxidant action include 3,3'-diselenodipropionic acid, binaphthylidiseleide and 3,3'-ditrifluoromethyldiphenyl diselenide.<sup>48</sup> These Se derivatives can be metabolized into different Se species, which can undergo further oxidation/reduction.<sup>7</sup> Our results however showed that the performance of DPDA is not satisfactory (Figure 9A). Our concentration dependent studies with a higher DPDA loaded



sample also showed a similar effect (not shown). ED and CVD Se showed higher toxicity. Even with the low release kinetics, the much better performance obtained with CVD Se suggests that the extent of Se release observed in this case was at a desirable level for cancer toxicity and/or that the Se adherent on the AAO surface also participated in killing cancer cells.

Notice that, the IC50 value of HA was found to be ~ 8.15 mM (Figure S8, Supplementary information). The IC50 value of HA was observed to be higher as compared to other Se species reported in previous studies.<sup>16,49</sup> This could be due to a combination of three possible reasons; (i) the different cell line used in our study, (ii) a different Se species/precursor utilised and (iii) the short survey time (6 h). However, the IC50 values reported here are not exclusive to our study, as similar values were previously reported by several other studies that utilised different cell lines.<sup>50,51</sup> A higher cell viability obtained for AAO loaded only with HA (Figure 9A) can be attributed to the high IC50 value. Interestingly, the addition of chitosan reduces cell viability, which is believed to be due to the inherent properties of chitosan, as discussed above.

The culture results in healthy osteoblast cells (Figure 9B) are also provided. Even though the % cell viability decreased in all the Se loaded AAO samples (when compared to control), the cell viability was always greater than 50 %. Comparatively higher cell viability obtained for ED Se can be due to the pre-deposited Au coating.

## Conclusions

Electrochemically engineered carriers based on nanoporous alumina loaded with Se were successfully prepared and their application in localized drug delivery for bone cancer treatment was demonstrated in principle. Several forms of Se, including inorganic Se ( $\text{H}_2\text{SeO}_3$ ), organic Se ( $(\text{C}_6\text{H}_5)_2\text{Se}$ ), metallic Se, electrodeposited (ED) Se and chemical vapour deposited (CVD) Se, as single delivery systems and their combination with chitosan and/or indomethacin as multi-drug delivery systems were prepared and explored. Their drug-loading, in-vitro drug-releasing performance and cancer cell toxicity were evaluated in order to assess their potential application in localized cancer therapy.

The drug-release results confirmed that all drug-carrier combinations could release Se, but the best results were obtained from chitosan-composites of inorganic, organic or metallic forms of Se. This combination is particularly favourable to provide sustained and controlled Se release from the nanoporous AAO carrier. Cross-sectional SEM images suggested that uniform thin film-like Se-chitosan is formed inside the pore walls, which provide enough space for a subsequent drug-loading. Similar release kinetics were observed when the drug was loaded simultaneously with Se-chitosan, implying the suitability of this system in designing multi-drug delivery systems for combination therapies. Finally, toxicity studies using cancer cells showed a decreased anti-cancer effect in the order: inorganic selenate > ED Se > CVD Se > metallic Se > organic Se. The work presented here thus suggests promising alternatives for localized delivery of Se using simple and low-cost drug-releasing implants.

## Acknowledgements

The authors acknowledge Endeavour Research Fellowship from Australian Department of Education to support VSS fellowship. The financial support from Australian Research Council (FT FT110100711 and DP120101680) is also acknowledged. We

thank members Losic Nano research group, School of Chemical Engineering, The University of Adelaide for their help during this study. The support from the technical staff from the Adelaide Microscopy, University of Adelaide, for providing SEM imaging facilities is acknowledged.

## Notes

<sup>a</sup>School of Chemical Engineering, University of Adelaide, Adelaide 5005, Australia.

E-mail: vssaji@hotmail.com; dusan.losic@adelaide.edu.au,

<sup>b</sup>Discipline of Orthopaedics and Trauma, University of Adelaide, Adelaide 5005, Australia

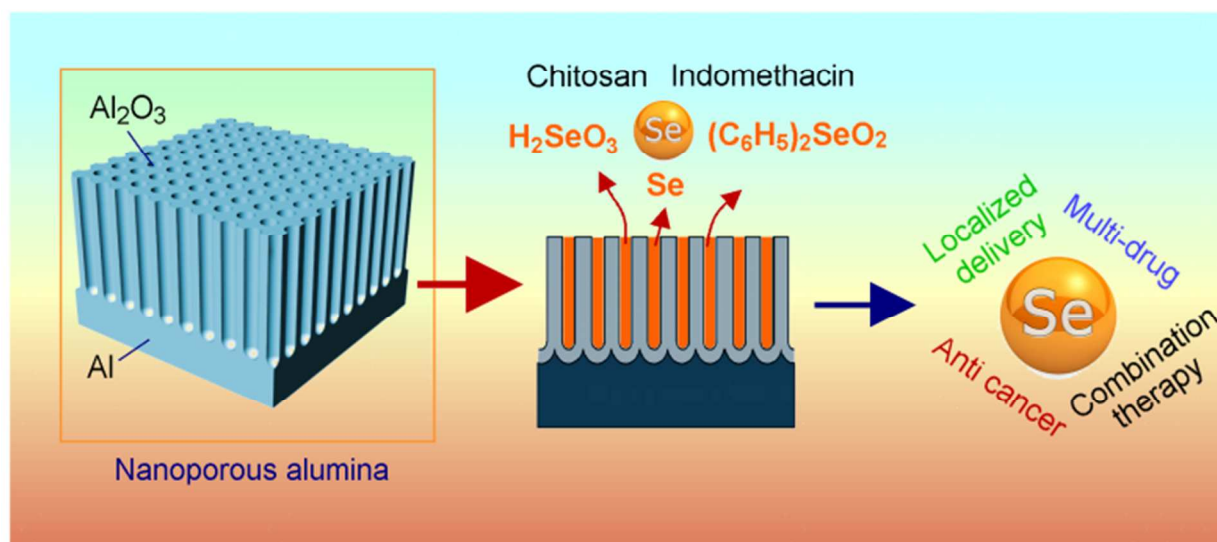
† Electronic Supplementary Information (ESI) available: Schematic showing advantages of Se addition, digital photographs of ED and CVD Se samples, selected area EDS spectrum of Se loaded AAO, representative TGA plot showing Se weight loss, BET curves of AAO before and after Se loading, UV-Vis spectra of different Se solutions, luminescence variation of CVD Se deposited AAO and IC50 value of HA are provided. See DOI: 10.1039/b000000x/

## References

- H. T. Ta, C. R. Dass, I. Larson, P. F. M. Choong and D. E. Dunstan, *Biomater.*, 2009, **30**, 3605.
- S. Ferrari, S. Smeland, M. Mercuri, F. Bertoni, A. Longhi, P. Ruggieri, T. A. Alvegard, P. Picci, R. Capanna, G. Bernini, C. Müller, A. Tienghi, T. Wiebe, A. Comandone, T. Böbling, A. B. Del Prever, O. Brosjö, G. Bacci and G. Sæter, *J. Clin. Oncol.*, 2005, **23**, 8845.
- V. S. Donnenberg, L. Zimmerlin, J. P. Rubin and A. D. Donnenberg, *Tissue Engineering B*, 2010, **16**, 567.
- J. R. Marshall and M. E. Reid, *Selenium in Encyclopedia of Cancer and Society*, ed. G. A. Colditz, Sage Publications, Inc., Thousand Oaks, 2007, pp. 785-788.
- H. Steinbrenner and H. Sies, *Biochim. Biophys. Acta*, 2009, **1790**, 1478.
- L. Flohé, Chapter 12, Selenium and Human Health: Snapshots from the Frontiers of Selenium Biomedicine, in *Selenium and Tellurium Chemistry*, ed. J. D. Woollins and R.S. Laitinen, Springer-Verlag Berlin Heidelberg, 2011, pp. 285-302.
- E. N. Drake, *Medical Hypotheses*, 2006, **67**, 318.
- M. E. Reid, A. J. Duffield-Lillico, E. Slate, N. Natarajan, B. Turnbull, E. Jacobs, G. F. Combs Jr, D. S. Alberts, L. C. Clark and J. R. Marshall, *Nutr. Cancer*, 2008, **60**, 155.
- H. -L. Seng and E. R. T. Tiekink, *Appl. Organomet. Chem.*, 2012, **26**, 655.
- M. Roman, P. Jitaru and C. Barbante, *Metallomics*, 2014, **6**, 25.
- P. Tran and T. J. Webster, *Int. J. Nanomedicine*, 2008, **3**, 391.
- F. Yang, Q. Tang, X. Zhong, Y. Bai, T. Chen, Y. Zhang, Y. Li and W. Zheng, *Int. J. Nanomedicine*, 2012, **7**, 835.
- W. Liu, X. Li, Y. -S. Wong, W. Zheng, Y. Zhang, W. Cao and T. Chen, *ACS Nano*, 2012, **6**, 6578.
- Y. Zhang, X. Li, Z. Huang, W. Zheng, C. Fan and T. Chen, *Nanomedicine*, 2013, **9**, 74.
- Y. Huang, L. He, W. Liu, C. Fan, W. Zheng, Y. -S. Wong and T. Chen, *Biomaterials*, 2013, **34**, 7106.
- B. Yu, X. Li, W. Zheng, Y. Feng, Y. -S. Wong and T. Chen, *J. Mater. Chem. B*, 2014, **2**, 5409.
- V. S. Saji and C. W. Lee, *RSC Adv.*, 2013, **3**, 10058.
- C. M. Weekley, J. B. Aitken, S. Vogt, L. A. Finney, D. J. Paterson, M. D. de Jonge, D. L. Howard, P. K. Witting, I. F. Musgrave and H. H. Harris, *J. Am. Chem. Soc.*, 2011, **133**, 18272.
- X. Chen, K. Cai, J. Fang, M. Lai, Y. Hou, J. Li, Z. Luo, Y. Hu and L. Tang, *Colloid Surf. B: Biointer.*, 2013, **103**, 149.
- J. Drews, *Science*, 2000, **287**, 1960.
- G. Jeon, S. Y. Yang and J. K. Kim, *J. Mater. Chem.*, 2012, **22**, 14814.

22. A. Santos, M. S. Aw, M. Bariana, T. Kumeria, Y. Wang and D. Losic, *J. Mater. Chem. B*, 2014, **2**, 6157.
23. M. S. Aw, M. Kurian and D. Losic, *Biomater. Sci.*, 2014, **2**, 10.
24. A. M. Md. Jani, D. Losic and N. H. Voelcker, *Prog. Mater. Sci.*, 2013, **58**, 636.
25. E. E. LearySwan, K. C. Popat, C. A. Grimes and T. A. Desai, *J. Biomed. Mater. Res. A*, 2005, **72**, 288.
26. K. E. La Flamme, K. C. Popat, L. Leoni, E. Markiewicz, T. J. La Tempa, B. B. Roman, C. A. Grimes and T. A. Desai, *Biomaterials* 2007, **28**, 2638.
27. H. -J. Kang, D. J. Kim, S. -J. Park, J. -B. Yoo and Y. S. Ryu, *Thin Solid Films*, 2007, **515**, 5184.
28. Y. Wang, A. Santos, G. Kaur, A. Evdokiou and D. Losic, *Biomaterials*, 2014, **35**, 5517.
29. H. Masuda and K. Fukuda, *Science*, 1995, **268**, 1466.
30. G. J. Atkins, K. J. Welldon, P. Halbout and D. M. Findlay, *Osteoporos. Int.*, 2009, **20**, 653.
31. G. J. Atkins, S. Bouralexis, A. Evdokiou, S. Hay, A. Labrinidis, A. C. W. Zannettino, D. R. Haynes and D. M. Findlay, *Bone*, 2002, **31**, 448.
32. C. P. Shah, C. Dwivedi, K. K. Singh, M. Kumar and P. N. Bajaj, *Mater. Res. Bull.*, 2010, **45**, 1213.
33. S. Kohara, S. Goldbach, N. Koura, M.-L. Saboungi, and L. A. Curtiss, *Chem. Phys. Lett.*, 1998, **287**, 282.
34. R. S. Oremland, M. J. Herbel, J. S. Blum, S. Langley, T. J. Beveridge, P. M. Ajayan, T. Sutto, A. V. Ellis and S. Curran, *Appl. Environ. Microbiol.*, 2004, **70**, 52.
35. B. Zare, S. Babaie, N. Setayesh and A. R. Shahverdi, *Nanomed. J.*, 2013, **1**, 13.
36. S. Dhanjal and S. S. Cameotra, *Microbial. Cell Factories*, 2010, **9**, 52.
37. Z. H. Lin and C. R. C. Wang, *Mater. Chem. Phy.* 2005, **92**, 591.
38. H. C. Akhmetov, Inorganic Chemistry, Translated from Russian by A. Rosinkin, MIR Publishers, Moscow, 1973, pp. 298-306.
39. T. Kumeria, M. M. Rahman, A. Santos, J. Ferré-Borrull, L. F. Marsal and D. Losic, *ACS Appl. Mater. Interfaces*, 2014, **6**, 12971.
40. J. Siepmann, F. Lecomte and R. Bodmeier, *J. Control. Release*, 1999, **60**, 379.
41. N. Bleiman and Y. G. Mishael, *J. Hazardous Mater.*, 2010, **183**, 590.
42. P. A. van den Brandt, M. P. Zeegers, P. Bode and R.A. Goldbohm, *Cancer Epidemiol. Biomarkers Prev.*, 2003, **12**, 866.
43. P. D. Whanger, *Br. J. Nutr.*, 2004, **91**, 11.
44. D. J. Waters, S. Shen, L. T. Glickman, D. M. Cooley, D. G. Bostwick, J. Qian, G. F. Combs Jr. and J.S. Morris, *Carcinogenesis*, 2005, **26**, 1256.
45. R. J. Shamberger, S. A. Tytko and C. E. Willis, *Arch. Environ. Health*, 1976, **31**, 231.
46. R. M. Rosa, D. J. Moura, A. C. R. E. Silva, J. Saffi and J. A. Pêgas Henriques, *Mutat. Res.*, 2007, **631**, 44.
47. R. Brandão, C. I. Acker, M. R. Leite, N. B. Barbosa and C. W. Nogueira, *J. Appl. Toxicol.*, 2009, **29**, 612.
48. D. Plano, Y. Baquedano, E. Ibáñez, I. Jiménez, J. Antonio Palop, J. E. Spallholz and C. Sanmartin, *Molecules*, 2010, **15**, 7292.
49. J. F. Ramos and T. J. Webster, *Int. J. Nanomed.*, 2012, **7**, 3907.
50. J. Y. Yang and Z. R. Wang, *Arch. Pharm. Res.*, 2006, **29**, 859.
51. S. Dwivedi, A. A. AlKhedhairy, M. Ahamed and J. Musarrat, *PLoS One*, 2013, **8**, e57404.

## Graphical Abstract



Release behavior and cancer toxicity of different forms of Se loaded into nanoporous AAO were studied.